Materials Physics and Mechanics 37 (2018) 184-191 Received: December 22, 2017

# INVESTIGATION OF THE FEATURES OF STRESS-STRAIN STATE IN LAYERED CYLINDRICAL CONSTRUCTIONS, MANUFACTURED OF TRANSVERSE-ISOTROPIC MATERIALS, UNDER PULSE IMPACT

**I.P. Miroshnichenko**

Don State Technical University, Gagarin Square 1, Rostov-on-Don, 344000, Russian Federation

e-mail: ipmir@rambler.ru

**Abstract.** The paper is devoted to the numerical study and analysis of the characteristics of the stress-strain state in layered cylindrical constructions made of transversely isotropic materials under pulsed loading with a given spatial-temporal distribution.
**Keywords:** layered cylindrical structure; a pulsed impact; the stress-strain state.

## 1. Introduction

Currently, the widespread use of anisotropic composite materials in the force elements of the constructions of different goods increases the importance of the study of the features of their stress-strain state, caused by wave processes under local pulsed loading. These loads arises both as in exploring the constructions, as in diagnostics of their state by active acoustic methods of nondestructive testing.

The paper [1] presents detailed specific examples of the numerical investigation of the stress-strain state in layered cylindrical structures made of transversely isotropic materials, subjected to pulse loads arising due to the curvature of the construction surface and physical-mechanical characteristics of the materials of layers.

The aim of this work is the numerical study and analysis of the stress-strain state in layered cylindrical constructions made of transversely isotropic materials under pulsed loading with a given spatial-temporal distribution.

## 2. Statement of problem: initial data and relationships

Let us consider the problem of determining the stress-strain state in layered cylindrical construction, referred to a cylindrical coordinate system (see Fig. 1). Pressure pulses are applied to some *j*-th regions of outer ($r = r_N$) the surface of the construction. The internal surface ($r = r_0$) is free of stresses ("free boundary"), and the interfaces of the layers ($r = r_n$; $n = 1,2,..., N-1$) rigidly fastened to each other ("hard bonding").

The layers made of a transversely isotropic material, the axes of symmetry of these layers coincide with the *z*-axis, and the design is assumed to be sufficiently long that corresponds to the radiation conditions at the construction edges.

The fields of displacements and stresses in each layer of the considered construction are described by the equations of motion [2] and should satisfy the boundary conditions.

We obtain the solution of this problem, based on the generalized method of the scalarization of dynamic elastic fields in transversely isotropic media [3]. It allows one to

http://dx.doi.org/10.18720/MPM.3722018_11

describe the searched fields by using three potential functions $\varphi$, $w$, $v$, corresponding to quasi-longitudinal, quasi-transverse and transverse waves and being solutions of the Helmholtz equations.

To find the full distributions of displacements and stresses, it is used spectral method. The pulse load $p(\theta, z, t)$ is present by its spectral density, which in the case of independence of the spatial-temporal distribution of the impact on the *z*-coordinate (non-axisymmetric case) has the form:

$$P(\theta,\omega) = \int_{-\infty}^{\infty} p(\theta,t)e^{i\omega t}dt\,, \tag{1}$$

where $\omega$ is the circular frequency.

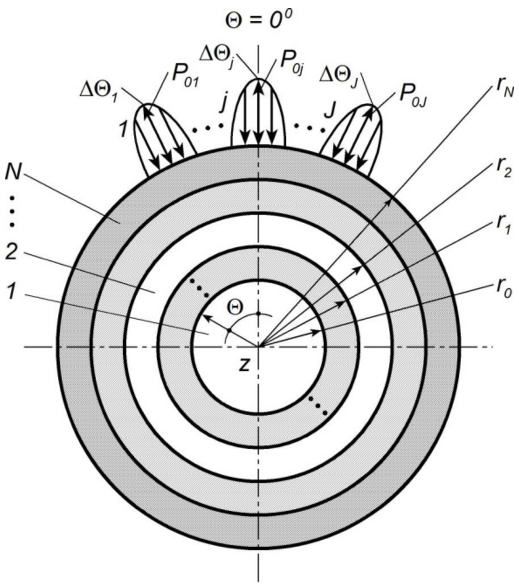


**Fig. 1.** Calculation scheme.

For example, under multipulse loading, if the distribution of each of the pressure pulses on coordinate $\theta$ has the semi-sine form, and the temporal dependence is given by the Gauss function, then the spectral density of this impact is defined as

$$P(\theta,\omega) = \sum_{j=1}^{J}\left[-p_{0j}\sqrt{\frac{\pi}{\beta_j}}e^{-\omega^2/4\beta_j}e^{i\omega t_j}\right]\left[a_{0j} + \sum_{m=1}^{M} a_{mj}\cos\{m(\theta+\Delta\theta_j)\}\right], \tag{2}$$

where $J$ is the number of pressure pulses; $p_{0j}$, $\tau_j$, $t_j$ are the amplitude, duration, and initial time of the action of the *j*-th pressure pulse, respectively;

$$\beta_j = \left(\frac{3.035}{\tau_j}\right)^2; \quad a_{oj} = \frac{\tau_{\theta j}}{\pi^2}; \quad a_{mj} = 2\pi\tau_{\theta j}[\sin(\pi x_{1j})/\pi x_{1j} + \sin(\pi x_{2j})/\pi x_{2j}];$$

$x_{1j} = \dfrac{m\tau_{\theta j}}{2\pi} - 0.5$; $x_{2j} = \dfrac{m\tau_{\theta j}}{2\pi} + 0.5$; $\tau_{\theta j}$ is the duration of the *j*-th pressure pulse in coordinate $\theta$; $\Delta\theta_j$ is the position of the *j*-th pressure pulse relatively of $\theta = 0$.

In non-axisymmetric case, the expressions for the displacements and stresses, which presence in the boundary conditions due to the functions $\varphi$ and $v$, have the forms:

$$U_r = \overset{(L)}{D_1}\frac{\partial\varphi}{\partial r} + \frac{1}{r}\frac{\partial v}{\partial\theta};$$

$$U_\theta = \overset{(L)}{D_1}\frac{\partial\varphi}{\partial\theta} - \frac{\partial\nu}{\partial r};$$

$$\sigma_{rr} = \overset{(L)}{d_1}\varphi + \overset{(L)}{d_4}\frac{\partial^2\varphi}{\partial r^2} + (C_{11} - C_{12})\left(\frac{1}{r}\frac{\partial^2\nu}{\partial r\partial\theta} - \frac{1}{r^2}\frac{\partial^2\nu}{\partial\theta^2}\right);$$

$$\sigma_{r\theta} = \overset{(L)}{d_4}\left(\frac{\partial\varphi}{\partial r\partial\theta} - \frac{1}{r^2}\frac{\partial\varphi}{\partial\theta}\right) + \frac{1}{2}(C_{11} - C_{12})\left(\frac{1}{r^2}\frac{\partial^2\nu}{\partial\theta^2} + \frac{1}{r}\frac{\partial\nu}{\partial r} - \frac{\partial^2\nu}{\partial r^2}\right), \quad (3)$$

where $\overset{(L)}{D_1} = \dfrac{\overset{(L)}{g}{}^2 b_4}{b_3 - \overset{(L)}{g}{}^2(1 - b_4)}$;

$b_3 = \omega^2\rho/C_{11}$; $b_4 = (C_{13} + C_{44})/C_{11}$;

$\overset{(L)}{d_1} = -\overset{(L)}{g}{}^2 a_1$; $\overset{(L)}{d_4} = 2a_2\overset{(L)}{D_1}$; $\overset{(T)}{d_3} = 2a_2\overset{(T)}{g} + 2a_4\overset{(T)}{g}$;

$a_1 = C_{12}$; $a_2 = (C_{11} - C_{12})/2$; $a_4 = C_{44} - (C_{11} - C_{12})/2$;

$C_{ij}$ are the moduli of elasticity.

The wave numbers $\overset{(L)}{g}$ and $\chi$ are defined as follows:

$$\overset{(L)}{g}{}^2 = A_1 - \sqrt{A_1^2 - A_2}; \; \chi^2 = 2\omega^2\rho/(C_{11} - C_{12}), \quad (4)$$

where $A_1 = (C_{11} + C_{44})\omega^2\rho/(2C_{11}C_{44})$; $A_2 = \omega^4\rho^2/(C_{11}C_{44})$; $\rho$ is the density.

The formulae (3) and (4), obtained from the constitutive relations [3, 4], taking into account the assumptions on the position of the axes of symmetry of the material layers and the limitations on external load.

The common solution of Helmholtz equations for functions $\varphi$ and $\nu$ is known:

$$\varphi = \sum_{m=0}^{\infty}\left[\varphi_m^+ H_m^{(1)}\left(\overset{(L)}{g} r\right) + \varphi_m^- H_m^{(2)}\left(\overset{(L)}{g} r\right)\right]\cos m\theta;$$

$$\nu = \sum_{m=0}^{\infty}\left[\nu_m^+ H_m^{(1)}(\chi r) + \nu_m^- H_m^{(2)}(\chi r)\right]\sin m\theta, \quad (5)$$

where $\varphi_m^+$, $\varphi_m^-$, $\nu_m^+$, $\nu_m^-$ are the amplitudes of the *m*-th harmonic of the corresponding types of waves, traveling in opposite directions across the layers; $H_m^{(1)}$ and $H_m^{(2)}$ are the Hankel functions of the 1st and 2nd kind of *m*-th order.

When we define the fields at certain point *r* for each harmonic $m$ and frequency $\omega$**,** then the following condition is checked:

$$\omega << v_l m/r, \quad (6)$$

where $v_l$ is the speed of quasi-longitudinal waves.

At violation of the condition (6), the functions $\varphi$ and $\nu$ are presented in the form of solutions of the Laplace equations:

$$\varphi = \left(\varphi_m^+ r^m + \varphi_m^- \frac{1}{r^m}\right)\cos(m\theta);$$

$$\nu = \left(\nu_m^+ r^m + \nu_m^- \frac{1}{r^m}\right)\cos(m\theta). \quad (7)$$

This is due to the instability of the solution, caused by the presence of the singularity of the Hankel function for small arguments in the low-frequency part of the spectrum and considering a large number of spatial harmonics in the description of the pressure pulses, localized in small areas on the construction surface, when the Hankel functions of high order are used.

The calculation relationships to determine the fields of displacements and stresses in each layer were obtained in matrix form, similarly to those described in [4], with a subsequent transition from conjugate space to real space by performing the inverse Fourier transform.

The absorption of wave energy by the materials of the layers was set by adding to the wave numbers $\overset{(L)}{g}$ and $\chi$ imaginary components, $\overset{(L)}{g}''$ and $\chi''$ being the absorption coefficients of the corresponding types of waves.

**3. Results of numerical modeling at multipulse loading with given spatial distribution**

By using the proposed method, we calculated distribution of the radial stresses $\sigma_{rr}(r,\theta)$ (see Fig. 2) in monolayer cylindrical structure ($r_1 = 1$ m; $r_0 = 0.1$ m; $\rho = 2700$ kg/m$^3$, $C_{11} = 107$ GPA; $C_{12} = C_{13} = 55.3$ GPA; $C_{44} = 25.9$ GPA; $\overset{(L)}{g}'' = 0.5$ m$^{-1}$; $\chi'' = 1$ m$^{-1}$) at time $t$, corresponding to the maximum amplitude for the given value $r$. These results were obtained on the outer surface of the construction at $r = r_1$ and at $r = 0.2$ m; upper and lower rows of plots in Fig. 2, respectively). Single pulse of pressure corresponds to Fig. 2 a, d and multiple pressure pulses with the duration of the $\tau = 2$ µs correspond to Fig. 2 b, c.

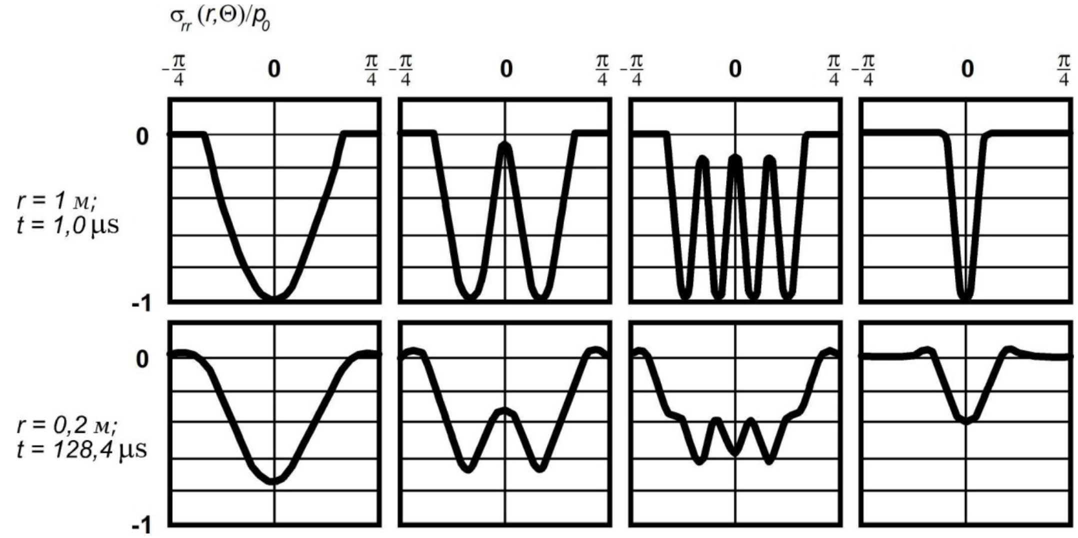


(a) (b) (c) (d)

**Fig. 2.** Distributions of radial stresses $\sigma_{rr}(r,\theta)$ in the coordinate $\theta$ in the cylindrical construction: (a) $\tau_{\theta 1} = \pi/3$, $\Delta\theta_1 = 0$; (b) $\tau_{\theta 1} = \tau_{\theta 2} = \pi/6$, $\Delta\theta_1 = \Delta\theta_2 = \pm\pi/12$; (c) $\tau_{\theta 1} = \tau_{\theta 2} = \tau_{\theta 3} = \tau_{\theta 4} = \pi/12$, $\Delta\theta_3 = \Delta\theta_4 = \pm\pi/8$; (d) $\tau_{\theta 1} = \pi/12$, $\Delta\theta = 0$.

The integration was carried out, using the method of fast Fourier transform at $K = 12$ ($2^K = 4096$ is the section number of partitioning the integration interval).

The distribution of the radial stresses $\sigma_{rr}(r,\theta)$, shown in Fig. 2, were obtained for: (a) $\tau_{\theta 1}=\pi/3, \Delta\theta_1=0$; (b) $\tau_{\theta 1}=\tau_{\theta 2}=\pi/6, \Delta\theta_1=\Delta\theta_2=\pm\pi/12$; (c) $\tau_{\theta 1}=\tau_{\theta 2}=\tau_{\theta 3}=\tau_{\theta 4}=\pi/12$, $\Delta\theta_3=\Delta\theta_4=\pm\pi/8$; (d) $\tau_{\theta 1}=\pi/12$, $\Delta\theta=0$.

Analysis of the simulation results (see Fig. 2) shows that at simultaneous loading by multiple pressure pulses, the pressure pulses with a small length $\tau_\theta$ expand and merge due to the diffraction, at the far distance from the place of the pulse application (the external surface of the construction). The stress amplitude in this case is close to the load amplitude of a single pressure pulse with a large $\tau_\theta$.

Figure 3 shows the distributions $\sigma_{rr}(\theta)$, obtained at the interface ($r=r_1$) of the layers in two-layered cylindrical construction ($r_2=0.5$ m; $r_1=0.2$ m; $r_0=0.1$ m) at different times $t$. These moments of time correspond to the maximum amplitudes at pulsed loading with parameters similar to shown in Fig. 2d (Fig. 3a) and Fig. 2c (Fig. 3b).

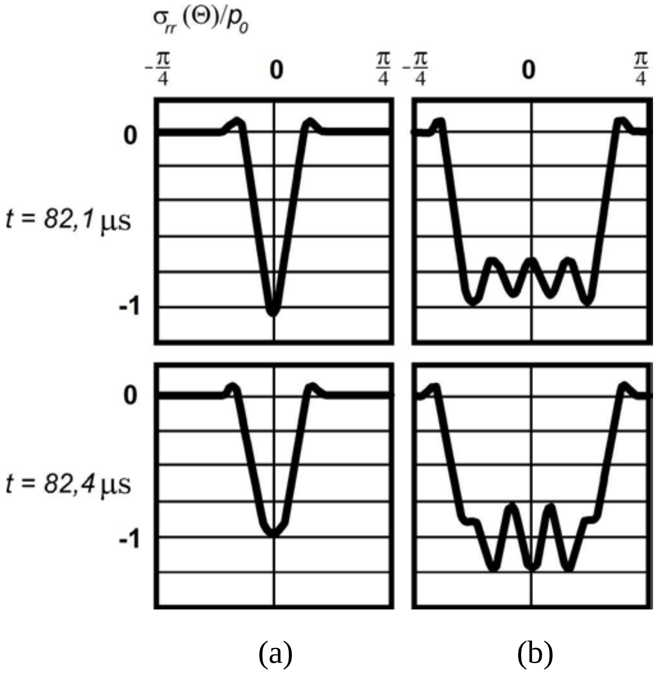


**Fig. 3.** Distributions of radial stresses $\sigma_{rr}(\theta)$ in the coordinate $\theta$ at the interface between layers ($r=r_1$) in two-layer cylindrical construction.

Physical-mechanical characteristics of the material of the inner layer coincided with those described above, and for the outer layer they had the following values: $\rho=1400$ kg/m$^3$; $C_{11}=19.2$ GPA; $C_{12}=C_{13}=8$ GPA; $C_{44}=5.6$ GPA; $\overset{(L)}{g}{}''=1$ m$^{-1}$; $\chi''=2$ m$^{-1}$.

Analysis of these distributions shows that due to the interference, the time, corresponding to the maximum amplitude at simultaneous loading by multiple pulses of pressure, occurs later than at loading by single pulse of pressure.

**4. Results of numerical modeling at multipulse loading with given temporal distribution**

We studied the stress-strain state at multipulse loading with a given temporal distribution by using the proposed method. The dependences of radial stress $\sigma_{rr}(t)$ were calculated at the interface between layers ($r=r_1$) in two-layer cylindrical construction ($r_2=1.2\cdot 10^{-2}$ m;

$r_1 = 6.0 \cdot 10^{-3}$ m; $r_0 = 3.0 \cdot 10^{-3}$ m, the relative thickness of the construction $\alpha = 0.75$, where $\alpha = (r_2 - r_0)/r_2$ [5]), at pulse loading (every pressure pulse is present in the form of the Gauss function with a duration of $\tau = 0.5$ μs with semi-sine shape on the outer surface ($r = r_2$) of a duration $\tau_\theta = \pi$, $\Delta\theta = 0$).

Physical-mechanical properties of materials of external and internal layers and the integration parameters coincide with the described in Section 3.

Figure 4 shows dependence of radial stress $\sigma_{rr}(t)$ at the interface between layers ($r = r_1$) in a two-layer cylindrical construction at loading by a single pulse of pressure in the form of the Gauss function. The upper part of the plot presents the temporal distribution of pulsed load on the outer surface of the construction ($r = r_2$).

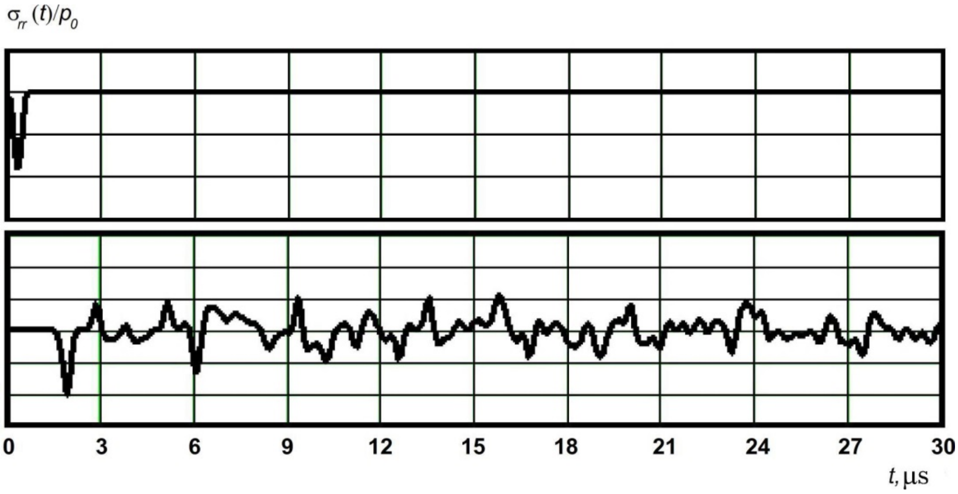


**Fig. 4.** Dependence of $\sigma_{rr}(t)$ at the interface between layers ($r = r_1$) in two-layer cylindrical construction at loading by single pulse of pressure in the form of Gauss function.

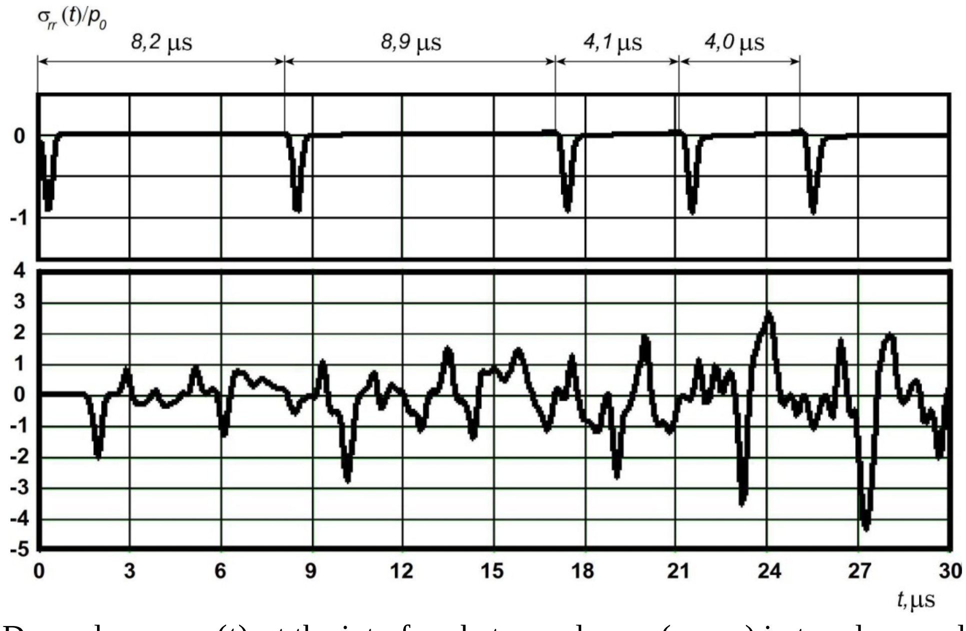


**Fig. 5.** Dependence $\sigma_{rr}(t)$ at the interface between layers ($r = r_1$) in two-layer cylindrical construction at repeated loading by pulses of pressure in the form of Gauss function.

Figure 5 shows the dependence of the radial stress $\sigma_{rr}(t)$ at the interface between layers ($r = r_1$) in two-layer cylindrical construction with repeated impacts of pressure pulses in the form of the Gauss function (5 identical pulses of pressure applied to the outer surface of the construction at time $t_1 = 0$ µs, $t_2 = 8.2$ µs, $t_3 = 17.1$ µs, $t_4 = 21.2$ µs, $t_5 = 25.2$ µs). The upper part of the plot presents the temporal distribution of pulsed impact on the outer surface of the construction ($r = r_2$).

The pointed temporal distribution of the pressure pulses is given in accordance with the recommendations of [5, 6], to achieve the maximum values of radial stresses $\sigma_{rr}(t)$ at the interface between layers ($r = r_1$) in the considered construction at limited number of pressure pulses. In this case, the pressure pulses were applied at intervals of time equal to the time intervals between maximum values of the radial stresses $\sigma_{rr}(t)$ of the same sign, obtained on dependence for the case of loading by a single pulse (see Fig. 4), but the order of application of these pulses must be reversed.

The analysis of these dependences shows that at a given temporal distribution of pulse impact, an increase by 4.3 times in the amplitude of the maximum radial stress takes place on the boundary of layers, compared to the maximum radial stress calculated for the case of single pulse of pressure.

The maximum amplitude of the radial stresses at the interface between layers of the construction may be increased up to 7.2 times compared to the maximum radial stresses, calculated for the case of single pulse of pressure, by using pressure pulses of rectangular shape instead of Gauss dependence.

Figure 6 shows dependence of change of radial stress $\sigma_{rr}(t)$ with time $t$ at the interface between layers ($r = r_1$) in a two-layer cylindrical structure at loading by pressure pulse of a rectangular shape, and Fig. 7 presents a similar dependence with repeated loading by pressure pulses of rectangular shape. The upper part of the plots presents the time distribution of pulsed load on the outer surface of the structure ($r = r_2$) for each of the calculated cases.

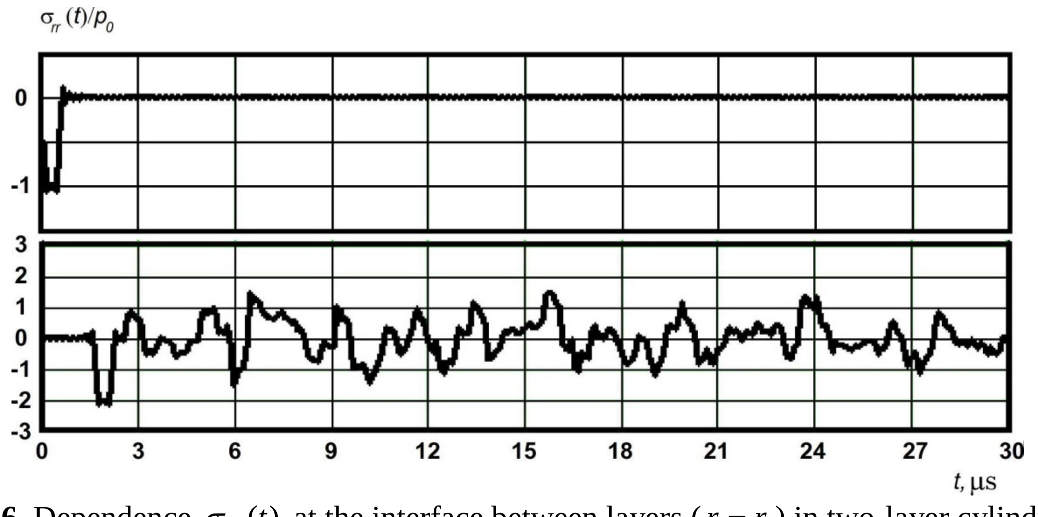


**Fig. 6.** Dependence $\sigma_{rr}(t)$ at the interface between layers ($r = r_1$) in two-layer cylindrical construction at loading by single pulse of pressure with rectangular shape.

The results of the numerical simulations clearly illustrate the features of the stress-strain state in layered cylindrical structures made of transversely isotropic materials under pulsed loading with a given spatial-temporal distribution and agree well with the results, published in the known papers, for example in [5, 6].

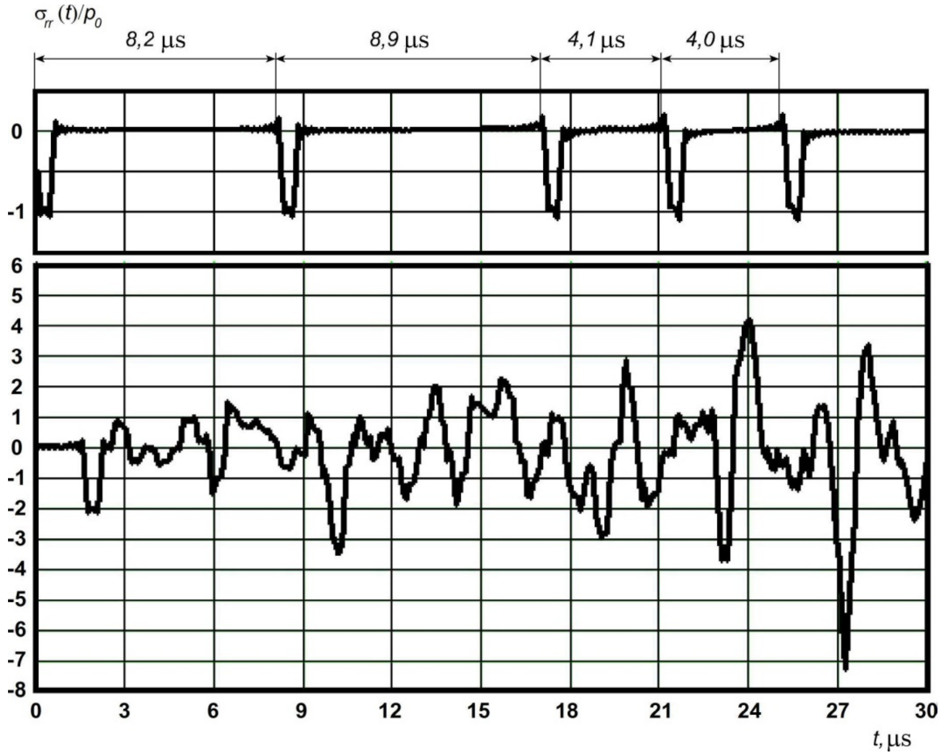


**Fig. 7.** Dependence $\sigma_{rr}(t)$ at the interface between layers ($r = r_1$) in two-layer cylindrical construction at repeated loading by pressure pulses of rectangular shape.

## 5. Conclusion

The results of calculations allow us to make conclusion on possibility of the application of developed method of calculating stress-strain state in layered cylindrical constructions, subjected to multiple local dynamic loads with high accuracy and taking into account the peculiarities of arising wave processes.

The above-described results is most appropriate to use at *a priori* and *a posteriori* analysis of the results of state diagnostics for advanced constructions made of new anisotropic layered composite materials, by using acoustic methods of nondestructive testing in mechanical engineering, shipbuilding, aircraft construction, etc.

***Acknowledgement.*** *This research is supported by the Ministry of Education and Science of the Russian Federation and grant of the Russian Foundation for Basic Research № 16-08-00740.*

## References

[1] I.P. Miroshnichenko, In: *Advanced Materials – Techniques, Physics, Mechanics and Applications. Springer Proceedings in Physics*, ed. by Ivan A. Parinov, Shun-Hsyung Chang, Muaffaq A. Jani (Springer Cham, Heidelberg, New York, Dordrecht, London, 2017), Vol. 193, p. 435.

[2] R.M. Christensen, *Mechanics of Composite Materials* (John Wiley & Sons, New York, 1979).

[3] V.P. Sizov // *Mechanics of Solids* **5** (1988) 55.

[4] V.P. Sizov, I.P. Miroshnichenko, *Excitation of Elastic Waves in Layered Anisotropic Structures* (LAP LAMBERT Academic Publishing, Saarbrucken, Germany, 2012).

[5] A.M. Petrov, V.P. Sizov // *Izvestiya VUZov. Mechanical Engineering* **2** (1985) 22.

[6] V.P. Sizov // *Izvestiya VUZov. Mechanical Engineering* **7–9** (1991) 33.